ARTICLE IN PRESS

Nature Communications

https://doi.org/10.1038/s41467-025-68260-9

Article in Press

Space-time superoscillations

Received: 5 May 2025

Accepted: 23 December 2025

Cite this article as: Shen, Y., Papasimakis, N., Zheludev, N.I. Space-time superoscillations. *Nat Commun* (2026). https://doi.org/10.1038/s41467-025-68260-9

Yijie Shen, Nikitas Papasimakis & Nikolay I. Zheludev

We are providing an unedited version of this manuscript to give early access to its findings. Before final publication, the manuscript will undergo further editing. Please note there may be errors present which affect the content, and all legal disclaimers apply.

If this paper is publishing under a Transparent Peer Review model then Peer Review reports will publish with the final article.

ARTICLE IN PRESS

© The Author(s) 2026. **Open Access** This article is licensed under a Creative Commons Attribution-NonCommercial-NoDerivatives 4.0 International License, which permits any non-commercial use, sharing, distribution and reproduction in any medium or format, as long as you give appropriate credit to the original author(s) and the source, provide a link to the Creative Commons licence, and indicate if you modified the licensed material. You do not have permission under this licence to share adapted material derived from this article or parts of it. The images or other third party material in this article are included in the article's Creative Commons licence, unless indicated otherwise in a credit line to the material. If material is not included in the article's Creative Commons licence and your intended use is not permitted by statutory regulation or exceeds the permitted use, you will need to obtain permission directly from the copyright holder. To view a copy of this licence, visit http://creativecommons.org/licenses/by-nc-nd/4.0/.

ARTICLE IN PRESS

Space-Time Superoscillation

Yijie Shen[1,2*], Nikitas Papasimakis[3], Nikolay I. Zheludev[3,4]

1. Centre for Disruptive Photonic Technologies, School of Physical and Mathematical Sciences, Nanyang Technological University, Singapore 637371, Singapore
2. School of Electrical and Electronic Engineering, Nanyang Technological University, Singapore 639798, Singapore
3. Optoelectronics Research Centre & Centre for Photonic Metamaterials, University of Southampton, Southampton SO17 1BJ, UK
4. Institute for Advanced Study, Texas A&M University, USA

* yijie.shen@ntu.edu.sg

Abstract

Superoscillation (SO) describes the ability of a band-limited electromagnetic wave to exhibit local oscillations in space or time that exceed the highest spatial or temporal Fourier component of the global wavefunction. SO has enabled light to be focused into arbitrarily small hotspots, forming the basis of superresolution imaging and metrology far beyond the Abbe-Rayleigh diffraction limit. Here we show that spatial and temporal superoscillations can occur simultaneously at the same point in space-time, a phenomenon we term space-time superoscillation (STSO). We demonstrate STSOs in band-limited supertoroidal light pulses, a recently introduced family of space–time nonseparable finite-energy solutions of Maxwell's equations. Our results reveal a new regime of extreme spatiotemporal field structuring, with implications for ultrafast metrology, light–matter interactions, and deep-subwavelength control of electromagnetic waves.

Introduction

Superoscillations (SOs) have emerged as a powerful concept in wave physics, enabling local oscillation rates that far exceed the maximum wavenumber present in the global spectrum [1,2]. This counterintuitive phenomenon—originally developed for monochromatic waves in one, two, or three dimensions—has inspired applications in optical superresolution imaging, precision metrology, and structured light engineering [1–5]. More recently, the concept has been extended to the temporal domain, revealing similarly surprising behaviour in ultrafast dynamics, spectroscopy, and light–matter interactions [6,7].

In parallel, advances in structured and nonseparable spatiotemporal fields have unlocked new degrees of freedom for shaping electromagnetic waves in both space and time [8–10]. Among these are supertoroidal pulses (STPs), a recently introduced class of exact solutions to Maxwell's equations that exhibit strong space–time nonseparability and rich topological structure [11]. A notable member of this family is the "Flying Doughnut" pulse—an experimentally demonstrated toroidal single-cycle waveform with tightly confined energy and nontrivial topology [12–15].

These developments raise a natural and fundamental question: Can spatial and temporal superoscillations coexist at the same space–time coordinates in a physically realizable, finite-energy electromagnetic pulse?

Here we show that STPs provide precisely such a platform. Their nonseparable geometry induces regions where both the local spatial wavevector and local temporal frequency far exceed the respective global spectral bounds. We term this phenomenon space–time superoscillation (STSO) and establish its existence analytically and numerically, revealing its key signatures and physical implications.

Results

ARTICLE IN PRESS

Supertoroidal pulse and band-limited formulations

An STP is characterized by two length parameters, q_1 and q_2, representing the effective wavelength and Rayleigh range, respectively, and a real dimensionless parameter α, which controls the pulse topology [11]. Finite-energy solutions require $\alpha \geq 1$; larger values of α yield increasingly rapid local field variations and stronger confinement [16]. STPs can be TE (transverse electric, azimuthally polarized) or TM (transverse magnetic, radially polarized). Here we focus on the TE case without loss of generality. The full field expressions are provided as:

$$E_\theta^{(\alpha)} = -2\alpha i f_0 \sqrt{\frac{\mu_0}{\varepsilon_0}} \left\{ \frac{(\alpha+1) r (q_1 + i\tau)^{\alpha-1} (q_1 + q_2 - 2ict)}{\left[r^2 + (q_1 + i\tau)(q_2 - i\sigma) \right]^{\alpha+2}} - \frac{(\alpha-1) r (q_1 + i\tau)^{\alpha-2}}{\left[r^2 + (q_1 + i\tau)(q_2 - i\sigma) \right]^{\alpha+1}} \right\} \tag{1}$$

$$H_r^{(\alpha)} = 2\alpha i f_0 \left\{ \frac{(\alpha+1) r (q_1 + i\tau)^{\alpha-1} (q_2 - q_1 - 2iz)}{\left[r^2 + (q_1 + i\tau)(q_2 - i\sigma) \right]^{\alpha+2}} - \frac{(\alpha-1) r (q_1 + i\tau)^{\alpha-2}}{\left[r^2 + (q_1 + i\tau)(q_2 - i\sigma) \right]^{\alpha+1}} \right\} \tag{2}$$

$$H_z^{(\alpha)} = -4\alpha f_0 \left\{ \frac{(q_1 + i\tau)^{\alpha-1} \left[r^2 - \alpha (q_1 + i\tau)(q_2 - i\sigma) \right]}{\left[r^2 + (q_1 + i\tau)(q_2 - i\sigma) \right]^{\alpha+2}} + \frac{(\alpha-1)(q_1 + i\tau)^{\alpha-2} (q_2 - i\sigma)}{\left[r^2 + (q_1 + i\tau)(q_2 - i\sigma) \right]^{\alpha+1}} \right\} \tag{3}$$

where (r, θ, z) are cylindrical coordinates, t is time, $c = 1/\sqrt{\varepsilon_0 \mu_0}$ is the speed of light, ε_0 and μ_0 are the permittivity and permeability of vacuum, $\tau = z - ct$, $\sigma = z + ct$, and f_0 is a normalizing constant. The instantaneous electric field can be written as $E_\theta(r, z, t) = A(r, z, t) e^{i\phi(r,z,t)}$, where A and ϕ correspond to the amplitude and phase, see detailed derivation in Supplementary Section S1. In the condition of propagation in vacuum without dispersion, the group velocity on axis (r=0) of the STPs of different orders is always the constant of c, see detailed proof in Supplementary Materials S1 around Eq. (S20), while the velocity of the centroid of the whole structured pulse is less than c.

Although STPs are localized finite-energy solutions to Maxwell's equatiosn, they are not exactly band-limited. To study SO behaviour, we therefore introduce band-limited STP, i.e. their versions with time domain and space domain spectra truncated at $\omega < \omega_m$ and $k < k_m = \omega_m/c$. Firstly, we obtain the spectrum of an STP field, $E(r, z, t)$, by Fourier transform from space-time (r, z, t) to spatiotemporal frequency (f_r, f_z, f) domain.

$$\tilde{E}(f_r, f_z, f) = \int_{-\infty}^{\infty} \int_{-\infty}^{\infty} \int_{-\infty}^{\infty} E(r, z, t) \exp\left[-i2\pi (f_r r + f_z z + ft) \right] dr dz dt \tag{4}$$

The entire spectrum of a space-time light pulse must be confined on the surface of light cone, i.e the conic surface with unit slope of its generatrix in the coordinate $(k_r, k_z, \omega/c)$, where the spatial wavevectors are related to the spatial frequencies by $k_r = 2\pi f_r/c$ and $k_r = 2\pi f_z/c$, and temporal frequency is related to the angular frequency by $\omega = 2\pi f$. We truncate STPs at a cut-off frequency, f_m, by multiplying their Fourier transform with a bump function $B(f)$ (see Supplementary Section S2 for details). The corresponding band-limited spatiotemporal STP pulse can be obtained by inverse Fourier transform:

$$\tilde{E}_c(r, z, t) = \int_{-\infty}^{\infty} \int_{-\infty}^{\infty} \int_{-\infty}^{\infty} \tilde{E}(f_r, f_z, f) B(f) \exp\left[i2\pi (f_r r + f_z z + ft) \right] df_r df_z df \tag{5}$$

Truncated STPs retain all the main features of their non-band-limited counterparts for $\omega_m \gg 4c/q_1$ (see details in Supplementary Material S2), including collocated spatial and temporal SOs.

ARTICLE IN PRESS

Coexistence of spatial and temporal superoscillation

We illustrate the presence of STSO, i.e. simultaneous spatial and temporal SOs, by considering an TE-mode STP with α=50, q_2=50q_1, q_1=1 (see Fig. 1a for the electric field distribution $E_\theta(r,z,t)$ in space-time, and Fig. 1b for the toroidal field isosurface structure). The spatial (radial) variation of the electric field along the radial direction at (z=0, t=t_s) is presented in Fig. 1c, where we observe that a segment in the off-axis region (r=r_s) oscillates considerably faster than the harmonic oscillation of the maximal radial frequency k_m (dashed red line). Similarly, in Fig. 1d, we show the temporal variation of the electric field at (z=0, r=r_s), which around t=t_s exhibits oscillations faster than the harmonic oscillation of maximal temporal frequency ω_m (dashed red line). Therefore, the field at focal plane (z=0) is both spatially and temporally superoscillatory at the point of space-time (r=r_s, t=t_s).

To further illustrate the emergence of STSOs in STPs, we consider their spatial and temporal distribution of the electric field at focus (z=0) for a fixed cut-off frequency ω_m=ck_m=2c/q_1. The field in SO region should have local wavevector (phase gradient) exceeding the global maximal wavevector (k_m) [1,17]. Figures 2(a1-a4) show the distribution of the logarithm of the electric field, i.e. $\log_{10}|\mathrm{Re}[E_\theta(r,z=0,t)]|$, unwrapped phase of $\phi(r,z=0,t)$, large phase gradient, energy and Poynting vector distributions, respectively, of the fundamental toroidal pulse (α=1). In Fig. 2(a3), there is only a small region with temporal local wavevector $\partial\phi/\partial r$ exceeding k_m, but no spatial SO and thus no STSO. This temporal SO is induced by the rapid cycle switching of the focused single-cycle pulse. In Fig. 2(a4), we also highlight the region of energy backflow accompanied by low amplitude values, in accordance with prior works [11,18]. Higher values of α lead to increasingly complex STPs with multi-cycle structure and dramatic spatiotemporal evolution, which results into an extreme spatiotemporal focusing effect with STSO. Figures 2(b1-b4) show the corresponding distribution of the logarithm of the electric field, unwrapped phase, large phase gradient regions, energy and Poynting vector distributions, for an STP with α=50. Figure 2(b3) shows the presence of spatial SOs, where the local wavevector exceeds k_m, and temporal SOs, where the local temporal frequency exceeds ω_m. Importantly, the spatial and temporal SOs overlap significantly indicating the presence of STSOs. We can also clearly observe that STSOs appear at low amplitude regions surrounded by higher-amplitude regions. Similar to the recently observed spatial SOs in the optical domain [18], STSOs are also accompanied by areas of energy backflow, see inset to Fig. 2(b4).

Scaling behaviour with the supertoroidal index

Figures 3(a) and 3(b) show temporal local wavevector profiles at specific radius r=10q_1 and spatial local wavevector profiles at specific time t=2q_1/c, respectively, for a series of STPs with varying value of parameter α. We observe that the spatial and temporal rapid oscillations become increasingly stronger with increasing α. Figure 3(c) shows the ratio between energy within the rapid oscillations region, E_{STSO}, and the total energy of the pulse, E_T, as a function of parameter α. We observe that for α>38, STSO behaviour emerges with the energy of STSOs monotonically increasing with increasing α, see Fig. 3(c). The fractional pulse energy contained within these regions increases monotonically with α, reaching values on the order of 10^{-3}–10^{-2} of the total pulse energy—within reach of current experimental detection methods [19–21].

Spectral signatures and off–light-cone components

A hallmark of SO is that local spectra contain frequency components that exceed the global band limit of the entire field [1]. Similarly, we demonstrate that the spectra of STSO segments of STPs contain components out of the light cone, i.e. they oscillate faster than what would be expected based on the pulse bandwidth. Figure 4 shows the entire spectra (a1-a4) and local spectra (b1-b4) and of STPs of different order, α = 1, 10, 50, and 100, defined as the Fourier transform of the local space-time segment $E_\theta(r\sim r_s,z=0,t\sim t_s)$ into the (k_r,ω) domain. The spectra of full pulses are confined on the surface of the light

ARTICLE IN PRESS

cone, whereas local spectra present spectral components outside the light cone. The presence of the off-light-cone components directly reveals the presence of STSOs. Whereas for the fundamental toroidal pulse (α=1), local spectra are fully contained within the light cone, in the case of the STPs (α>1) the off-cone components become stronger with increasing value of α. This provides direct evidence that the field locally oscillates faster than permitted by its global spectral support. These off-cone components strengthen dramatically with increasing α, in parallel with the observed STSO enhancement.

Discussion

The STSOs predicted here are accessible with present-day technology. Optical, THz, and microwave platforms have already demonstrated generation of fundamental toroidal pulses and complex hybrid toroidal pulses [13-15,21]. For an estimate in the optical domain, a Ti:Sa laser with a $\Delta\lambda$ = 200 nm bandwidth (FWHM) central at λ_0 = 800 nm yields spatial and temporal focusing limits of $\lambda_0/2$ = 400 nm and $\Delta\tau = \frac{K\lambda_0^2}{c\Delta\lambda}$ = 4.64 fs (constant K=0.441 for Gaussian profile pulse), respectively. Based on the results in Fig. 3(a,b), for STP of α=100, at STSO spot, the temporal and spatial local wavevectors are about 7 and 5 times larger than the central wavevector, respectively. implying achievable hotspots temporal and spatial confinements of about $\Delta\tau/7$=0.66 fs and $\lambda_0/2/5$ = 80 nm. Here, we evaluate central wavevector as k_c=1 (unit: $1/q_1$) as the central wavevector, it actually is less than 1, see Fig. 4a. Isolated temporal peaks can be even more extreme (the central peak of Figs. 3(a) over 45 times than k_c=1), potentially reaching sub-100-as effective confinement.

The energy content of STSO regions (~0.1–1% of total energy, see Fig. 2b and Fig. 3c) is comparable to or higher than that successfully exploited in prior SO-enabled microscopy, metrology, and wavefront-shaping experiments [6,7,19,20]. For instance, in SO super-microscope experiment [19], by applying the center SO hot spot about 0.1% energy of the total energy of the whole field, we can already enable the effective microscope, as the outside high-energy lobs were actually filtered out. Established techniques for detecting weak high-spatial-frequency features in the presence of strong sidelobes are therefore directly applicable.

Our findings expand the superoscillation paradigm by demonstrating that simultaneous spatial and temporal superoscillations are physically realizable in finite-energy electromagnetic pulses. Further, our work invites key questions about the underlying physics of electromagnetic STSOs:

- What physical mechanisms or field-topological constraints govern the emergence of STSOs?
- Is space–time nonseparability a necessary condition, or merely a sufficient one?
- Can a canonical synthesis formalism be developed—analogous to angular spectrum methods—for designing optimal STSO fields?

Moreover, the STSO spots demonstrated above are in isolated form, which are possible to be extended into more complex structured form, such as STSO spot array and multi-lobe forms. For instance, we can linearly superimpose a pulse chain of many STSOs to generate SO spatiotemporal arrays, analogous to the previous methods to produce multi-lobe SO arrays in the spatial domain [22,23].

The applications of STSOs should be clear and highly anticipated, as spatial temporal SOs have enabled important applications individually. In particular, spatial SOs have recently led to superresolution metrology even with picometric resolution [24,25], microscopy and imaging [1,19,20], while temporal SOs are finding applications in advanced spectroscopies [7]. Therefore, by combining for the first time these two forms of SOs into STSOs, we anticipate applications in metrology, imaging, sensing, and spectroscopy

ARTICLE IN PRESS

at ultra-fine spatial and ultrafast temporal resolution. Further, STSOs in light pulses pave the way towards novel phenomena arising from the coupling between STSO pulses and novel materials, e.g. controlling the spatiotemporal dynamics of phonons via the STSO light field [26]. Moreover, STSOs emerge in regions of rapid field reversal resulting from a nested skyrmionic topological structure [11], which can also be extended with nondiffracting robust propagation [27]. Recently, optical skyrmions found their applications in subwavelength sensing, metrology, and light-matter interaction [28-30], therefore, we perspective the skyrmions with SO and STSO has potential to further enhance the deep-subwavelength resolution in these applications.

Although demonstrated here for electromagnetic waves, the underlying mechanism is universal. We anticipate that STSO behavior may be found in other spatiotemporally structured light fields, not limited to the STPs considered here. Any wave system supporting structured, finite-energy, space–time nonseparable solutions—acoustic, elastic, water, or gravitational waves—should in principle exhibit STSO behaviour. This broadens the potential impact of STSOs far beyond photonics.

ARTICLE IN PRESS

References

1. N. I. Zheludev and G. Yuan, Optical superoscillation technologies beyond the diffraction limit *Nat. Rev. Phys.* **4**, 16-32 (2022).
2. Chen, G., Wen, ZQ. & Qiu, CW. Superoscillation: from physics to optical applications *Light Sci Appl* **8**, 56 (2019).
3. M. V. Berry and S. Popescu, Evolution of quantum superoscillations and optical superresolution without evanescent waves *J. Phys. A* **29**, 6965 (2006).
4. M V Berry, Superoscillations for monochromatic standing waves*J. Phys. A: Math. Theor.* **53** 225201 (2020)
5. M. V. Berry and M. R. Dennis, Natural superoscillations in monochromatic waves in D dimensions *J. Phys. A: Math. Theor.* **42**, 022003 (2009).
6. Y Eliezer, L Hareli, L Lobachinsky, S Froim, and A Bahabad, Breaking the Temporal Resolution Limit by Superoscillating Optical Beats *Phys. Rev. Lett.* **119**, 043903 (2017)
7. G. McCaul, P. Peng, M. O. Martinez, D. R. Lindberg, D. Talbayev, and D. I. Bondar, Superoscillations Deliver Superspectroscopy *Phys. Rev. Lett.* **131**, 153803 (2023).
8. Yessenov, M., Hall, L. A., Schepler, K. L., & Abouraddy, A. F., Space-time wave packets *Adv. Opt. Photon.* **14**(3), 455-570 (2022).
9. Y. Shen *et al* 2023 Roadmap on spatiotemporal light fields *J. Opt.* **25** 093001.
10. Liu, X., Cao, Q., & Zhan, Q. Spatiotemporal optical wavepackets *Photonics Insights* **3**(4), R08-R08 (2024).
11. Y. Shen, Y. Hou, N. Papasimakis, and N. I. Zheludev, Supertoroidal light pulses as electromagnetic skyrmions propagating in free space *Nat. Commun.* **12**, 5891 (2021).
12. R. W. Hellwarth and P. Nouchi, Focused one-cycle electromagnetic pulses *Phys. Rev. E* **54**, 889–895 (1996).
13. A. Zdagkas, C. McDonnell, J. Deng, Y. Shen, G. Li, T. Ellenbogen, N. Papasimakis, and N. I. Zheludev, Observation of toroidal pulses of light *Nat. Photonics* **16**, 523–528 (2022).
14. K. Jana, Y. Mi, S. H. Møller, D. H. Ko, S. Gholam-Mirzaei, D. Abdollahpour, S. Sederberg and P. B. Corkum, Quantum control of flying doughnut terahertz pulses *Sci. Adv.* **10**, eadl1803 (2024).

ARTICLE IN PRESS

15. R. Wang, P.-Y. Bao, Z.-Q. Hu, S. Shi, B.-Z. Wang, N. I. Zheludev, Y. Shen, Observation of resilient propagation and free-space skyrmions in toroidal electromagnetic pulses *Appl. Phys. Rev.* **11**, 031411 (2024).
16. Ziolkowski, Localized transmission of electromagnetic energy, Phys. Rev. A 39, 2005 (1989)
17. M V Berry, Five momenta, Eur. J. Phys. 34 (2013) 1337–1348.
18. Yuan, G., Rogers, E.T.F. & Zheludev, N.I. "Plasmonics" in free space: observation of giant wavevectors, vortices, and energy backflow in superoscillatory optical fields. *Light Sci Appl* 8, 2 (2019).
19. Wong, A., Eleftheriades, G. An Optical Super-Microscope for Far-field, Real-time Imaging Beyond the Diffraction Limit. *Sci Rep* **3**, 1715 (2013)
20. Rogers, E., Lindberg, J., Roy, T. *et al.* A super-oscillatory lens optical microscope for subwavelength imaging. *Nature Mater* **11**, 432–435 (2012)
21. R. Wang, B. Ying, S. Shi, J. Wang, B.-Z. Wang, M. Liang, and Y. Shen, "Hybrid electromagnetic toroidal vortices," *Sci. Adv.* **11**, eads4797 (2025)
22. Z. Deng, N. Shapira, R. Remez, Y. Li, and A. Arie, Talbot effect in waveforms containing subwavelength multilobe superoscillations. *Opt. Lett.* **45**, 2538–2541 (2020)
23. Lim, S.W.D., Park, JS., Kazakov, D. *et al.* Point singularity array with metasurfaces. *Nat Commun* **14**, 3237 (2023)
24. G. H. Yuan, N. I. Zheludev, Detecting nanometric displacements with optical ruler metrology *Science* **364**, 771-775 (2019)
25. Liu, T., Chi, CH., Ou, JY. *et al.* Picophotonic localization metrology beyond thermal fluctuations. *Nat. Mater.* **22**, 844–847 (2023)
26. Afanasiev, D., Hortensius, J.R., Ivanov, B.A. *et al.* Ultrafast control of magnetic interactions via light-driven phonons. *Nat. Mater.* **20**, 607–611 (2021)
27. Shen, Y., Papasimakis, N. & Zheludev, N.I. Nondiffracting supertoroidal pulses and optical "Kármán vortex streets". *Nat Commun* **15**, 4863 (2024).
28. Y. Shen, Q. Zhang, P. Shi, L. Du, X. Yuan, A. V. Zayats, "Optical skyrmions and other topological quasiparticles of light," *Nat. Photonics* **18**, 15–25 (2024).
29. Y. Shen, H. Wang, and S. Fan, "Free-space topological optical textures," *Adv. Opt. Photonics* **17**(2) 295-374 (2025)
30. R. Wang, P.-Y. Bao, X. Feng, J. Wu, B.-Z. Wang, and Y. Shen, "Single-antenna super-resolution positioning with nonseparable toroidal pulses" *Commun. Phys.* **7**, 356 (2024)

Data Availability

The data from this paper can be obtained from the University of Southampton ePrints research repository at https://doi.org/10.5258/SOTON/XXXX (will provide before eProof stage)

Code Availability

The code from this paper and details on the code used can be obtained from the University of Southampton ePrints research repository https://doi.org/10.5258/SOTON/XXXX (will provide before eProof stage).

Competing interests

The authors declare no competing interests.

Acknowledgements

ARTICLE IN PRESS

The UKs Engineering and Physical Sciences Research Council (grant EP/T02643X/1, Funder Id: 10.13039/501100000266), the European Research Council (Advanced grant FLEET-786851 & Proof of Concept Grant ASTRA-101248385, Funder Id: https://doi.org/10.13039/501100000781), the Defense Advanced Research Projects Agency (DARPA) under the Nascent Light Matter Interactions program, Singapore MOE AcRF Tier 1 grants (RG157/23 & RT11/23), Singapore Agency for Science, Technology and Research (A*STAR) MTC Individual Research Grants (M24N7c0080), and a Nanyang Assistant Professorship Start Up grant.

Author Contributions

Y.S, N.P. and N.I.Z. conceived the idea of the research. Y.S. performed the theoretical simulations and created graphical illustrations. All authors contributed to the manuscript preparation and discussion of results.

ARTICLE IN PRESS

Figures

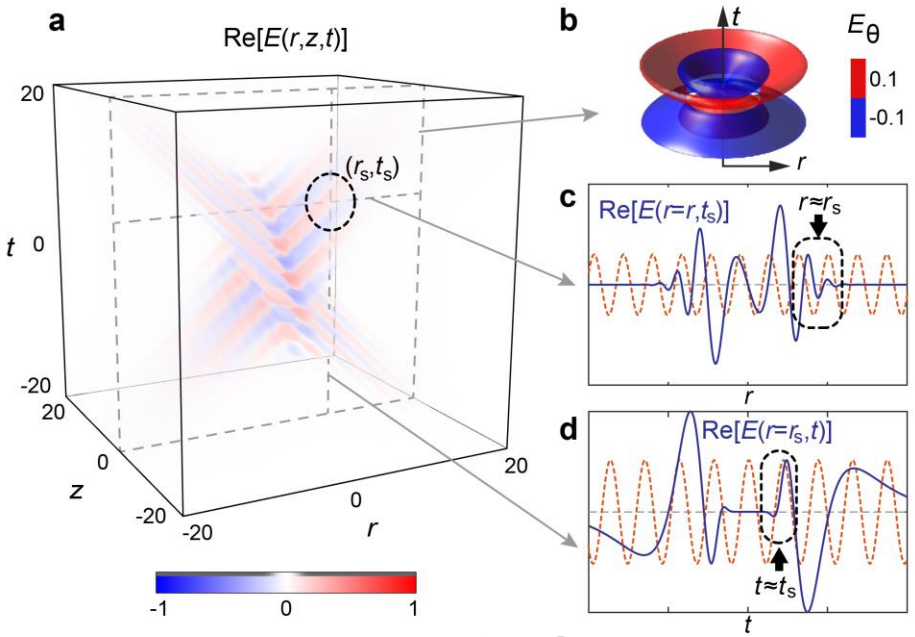

Figure 1: **Superoscillations in a band-limited supertoroidal light pulse** (α=50, q_2=50q_1). **a,** Spatiotemporal evolution of the azimuthal electric field, $E_\theta(r,z,t)$. **b,** Isosurfaces of the electric field, $E_\theta(r,z=0,t)$, in the focal plane. **c,d,** Radial (c) and temporal (d) field profiles at focus (z=0) at specific moment in time t_s=5 (c, blue line), and at specific radial position r_s=10 (d, blue line), respectively. The corresponding fastest spatial (c) and temporal (d) Fourier components are marked by red-dashed lines. The black dashed boxes highlight the SO region. Unit for length: q_1, Unit for time: q_1/c.

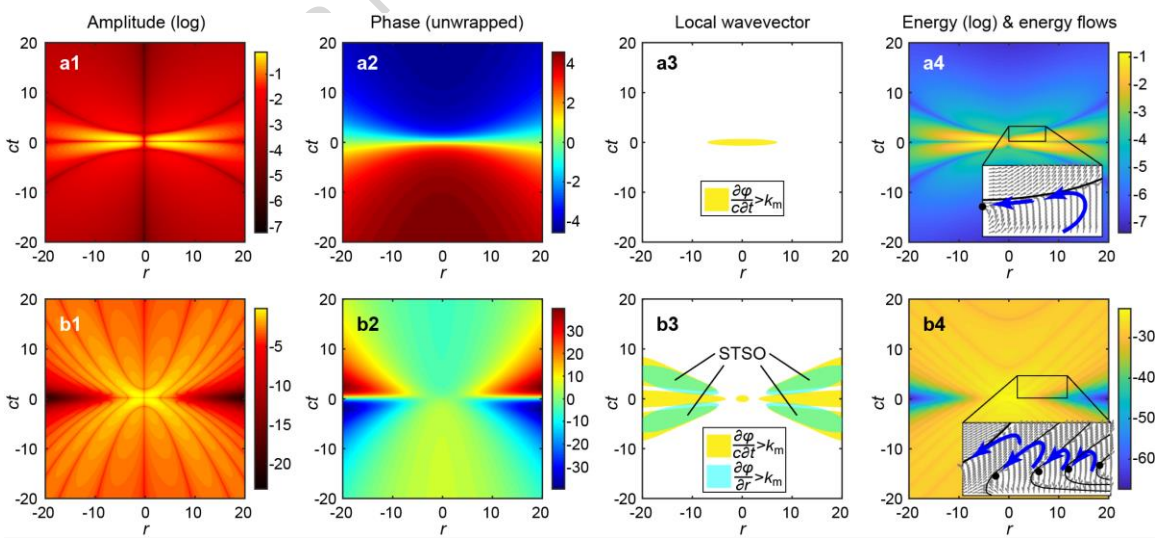

Figure 2: **Characterizations of toroidal and supertoroidal pulses. a1,b1**, Spatiotemporal field modulus ($|E_\theta(r,z=0,t)|$) distributions for a toroidal pulse (α=1) (**a1**) and an STP (α=50) (**b1**), at focus (z=0). The amplitude is presented in terms of the logarithm of its real part, $\log_{10}|\mathrm{Re}[E_\theta(r,z=0,t)]|$. **a2,b2**, Unwrapped phase distributions $\varphi(r,t)=\mathrm{Arg}[E_\theta(r,z=0,t)]$ of the two pulses presented in (a1,b1). **a3,b3**, Regions in which the radial local wavevector ($\partial\varphi/\partial r$) and local temporal frequency ($\partial\varphi/\partial t$) of the

toroidal (a3) and supertoroidal (b3) pulse exceed the threshold frequency, ω_m, and wavevector, k_m, respectively ($k_m=2/q_1$). **a4,b4**, The energy spatial and temporal distribution, $w=(\epsilon_0 E^2+\mu_0 H^2)/2$, for the two pulses. Insets show the local energy flow with the black solid lines and dots marking the zero lines and singularities, and blue thick arrows marking the areas of energy backflow. Unit for all axes, r and ct, is q_1.

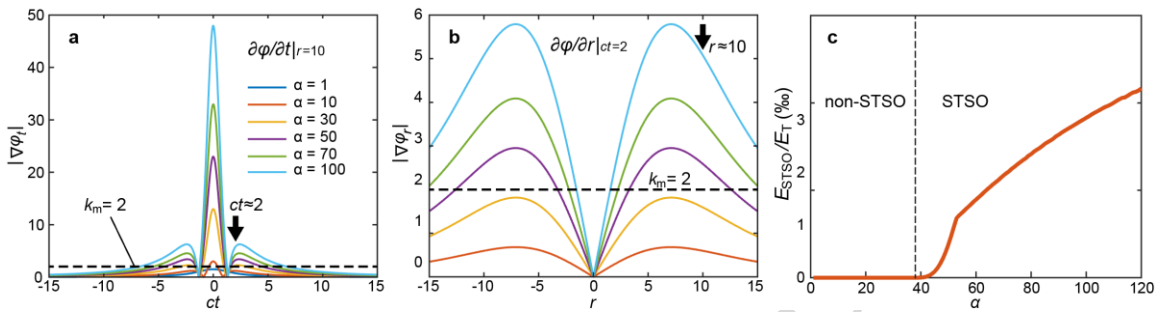

Figure 3: **Characterizing space-time superoscillations. a,b**, The temporal local frequency at r=10 (**a**) and the radial local wavevector at t/c=2 (**b**) of supertoroidal pulses for different values of α. The black dashed lines mark the value of the fastest spatial and temporal frequency component, respectively. **c**, the ratio of energy in the STSO region over the total energy of the pulse as a function of supertoroidal order α.

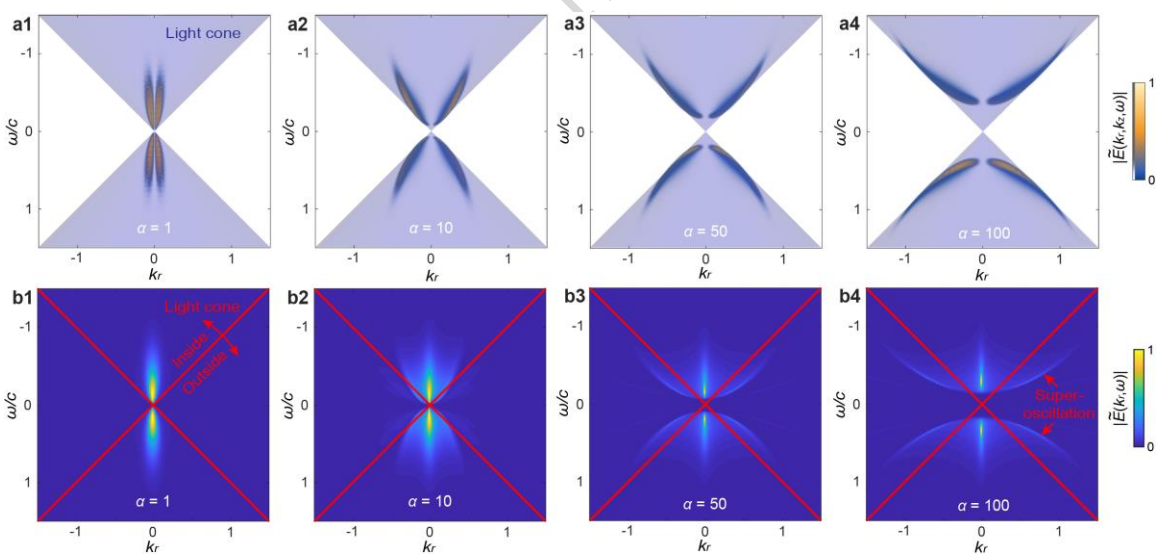

Figure 4: **Spectral characterizations. a1-a4**, Entire spectral power projected in the (k_r,ω) plane for toroidal pulses (α=1) and STPs (α=10, 50, 100). The light blue regions mark the light cone. **b1-b4**, Local spectral power in the (k_r,ω) plane corresponding to radial-temporal STSO segments of pulses of different order (α=1, 10, 50, 100). The red lines mark the boundary of the light cone. Note that, whereas the spectra of the full pulses (a1-a4) are confined on the surface of the light cone, local segments (b1-b4) exhibit out-of-cone components. Unit: $1/q_1$

ARTICLE IN PRESS

Editor Summary:

Superoscillations enable waves to oscillate faster beyond classical limits. Here, the authors demonstrate simultaneous spatial and temporal superoscillations in structured light pulses, achieving extreme both subwavelength and ultrafast focusing in space-time.

Peer Review Information:

Nature Communications thanks anonymous reviewers for their contribution to the peer review of this work. [A peer review file is available.]

ARTICLE IN PRESS